

New chelation products of thorium(IV) and cerium(III) with diclofenac and paracetamol analgesic drugs: Synthesis, spectroscopic, thermal stability, antimicrobial activities investigations

F.A.I. Al-Khodir

College of Science, Princess Nourah bint Abdulrahman University, Department of Chemistry, KSA

Received, November, 26, 2017; Revised, December, 21, 2017

Four new complexes of thorium(IV) and cerium(III) with two analgesic drugs, diclofenac sodium (*diclo*) and paracetamol (*para*): $[\text{Ce}(\text{diclo})_3] \cdot 2\text{H}_2\text{O}$ (1), $[\text{Th}(\text{diclo})_2(\text{OH})_2] \cdot 4\text{H}_2\text{O}$ (2), $[\text{Ce}(\text{para})_3(\text{H}_2\text{O})_3]$ (3), and $[\text{Th}(\text{para})_4(\text{H}_2\text{O})_2]$ (4), were synthesized and characterized using elemental analysis, thermal analysis and FT-IR, $^1\text{H-NMR}$, and UV-VIS spectroscopy. The micro-analytical elemental measurements confirmed the ratio metal ions:drug for the synthesized complexes as 1:3 for complexes 1 and 3, 1:4 for complex 2, and 1:2 for complex 4. The FT-IR spectra of the *para* ligand $\nu_s(\text{O-H})$ stretching vibration of $-\text{OH}$ disappeared in the spectra of the complexes proving the involvement of the oxygen atom of the $-\text{OH}$ group in the complexation after deprotonation. In case of *diclo* complexes, the $\nu(\text{C=O})$ stretching vibrations of the carboxylic group were shifted in the spectra of the complexes, confirming the involvement of the $-\text{COOH}$ group in the complexation with covalent bonding as bidentate chelation. The geometry of the Ce^{3+} and Th^{4+} ions was six-coordinated with those of both drug complexes. The nano-structured form was investigated using transmittance electron microscope (TEM). The antimicrobial activities of the newly synthesized complexes were determined against some kinds of bacteria and fungi. All these complexes showed antimicrobial results.

Keywords: Thorium(IV); Cerium(III); TEM; Nanoscale; Diclofenac; Paracetamol; IR.

INTRODUCTION

Diclofenac sodium (*diclo*, Fig. 1) is a sodium salt of aminophenyl acetic acid and is a well-known representative of non-steroidal anti-inflammatory drugs (NSAIDs) [1,2]. Like other NSAIDs diclofenac sodium is clinically prescribed as an antipyretic, analgesic and anti-inflammatory agent [3-5]. Knowledge of the structure of *diclo* molecule is essential to understand its pharmaceutical action. The *diclo* is a potent inhibitor of cyclo-oxygenase *in vitro* and *in vivo*, therapy decreasing the synthesis of prostaglandins, prostacyclin, and thromboxane products. Lanthanide ion probe spectrofluorometry (LIPS) introduced by Horrocks and Sundick [6] employs this technique for determination of diclofenac sodium. The structure of diclofenac consists of phenylacetic acid group, secondary amino group, phenyl ring, both *ortho* position of which are occupied by chlorine atom. The secondary amino group precipitates in bifurcate intramolecular hydrogen bond interacting with the adjacent acceptor chlorine atom [7-9]. The interaction of diclofenac with cyclodextrin has been reported [9,10]. The nature of the inclusion complex in the solid state was studied by X-ray crystallography, IR, and NMR spectroscopy.

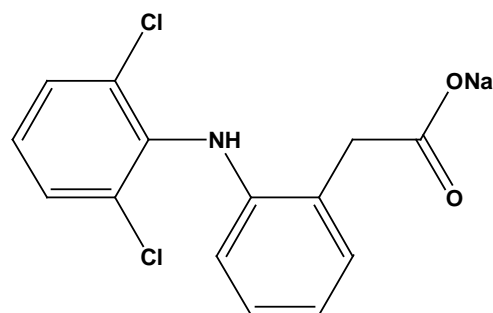


Fig. 1. Chemical structure of diclofenac sodium (*diclo*).

Paracetamol (*para*, Fig. 2) is a well-known drug that has application in pharmaceutical industries as a popular analgesic and antipyretic medication that is readily absorbed after administration and little toxic when used in recommended dose [11-17].

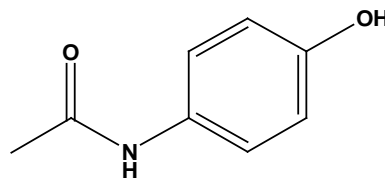


Fig. 2. Chemical structure of paracetamol (*para*).

Paracetamol in pharmaceutical preparations can be determined by different methods such as fluorimetry [18], chemiluminescence [19], electrochemical method [20], nuclear magnetic resonance, mass spectroscopy [21], and liquid chromatography [22]. Paracetamol has high therapeutic value; it is also used as an intermediate

* To whom all correspondence should be sent.
E-mail: fatimaalkhodir@yahoo.com

for pharmaceuticals (as a precursor of penicillin) and azo dye, stabilizer for hydrogen peroxide, photographic chemical [23]. Paracetamol is also known to be hepatotoxic in man and various experimental animals upon overdose [24]. Paracetamol is also oxidized by cytochrome P450 into the reactive intermediate N-acetyl-p-benzoquinone imine [25]. Several different approaches have previously been utilized in an attempt to achieve rapidly absorbed solid dose paracetamol formulations. These include enhancing tablet disintegration rate [26], addition of alkali metal salt or antiacid [27] to paracetamol tablets.

In the present work, we focused on raising the efficiency of the drug by the addition of a special metal ion like Ce^{3+} and Th^{4+} and formation of new complexes, to be proven using thermal and spectroscopic characterizations. These complexes were structurally characterized in the solid state by IR, 1H -NMR, conductivity measurement, thermal studies and biological evaluation. The nanoscale range of drug complexes was investigated using transmission electron microscopy (TEM).

EXPERIMENTAL

Chemicals and reagents

The analgesic drugs diclofenac sodium (*diclo*) and paracetamol (*para*) were purchased from Merck, all the other used reagents and solvents were analytical grade products. Hydrated salts of both $Th(NO_3)_4$ and $CeCl_3$ were obtained from Aldrich Company.

Synthesis of Ce^{3+} and Th^{4+} complexes

Ce(III) and Th(IV) complexes of diclo drug. The mentioned complexes were prepared as follows, employing a molar ratio (metal:drug) of 1:3 and 1:4 for $Ce(III)$ and $Th(IV)$ complexes, respectively. The resulting solutions were stirred and refluxed on a hot plate at 60-70°C for 3 h. The volume of the obtained solution was reduced to one-half by evaporation one day later, the precipitates were settled down, filtered off and washed several times by small amounts of hot CH_3OH and dried under *vacuum* over anhydrous $CaCl_2$. The data from the elemental analysis (Table 1) were in good agreement with those corresponding to the formula.

Ce(III) and Th(IV) complexes of para drug. $Th(IV)$ nitrate or $Ce(III)$ chloride (1 mmol) were dissolved in 20 mL of distilled water and then were added to 20 mL of methanolic solution containing 4 mmol of *para* under magnetic stirring. The pH of solution was adjusted to neutral using ammonium hydroxide solution. The resulting mixture was heated to 60 °C and left to evaporate slowly at room

temperature. The precipitate was filtered off, washed with hot methanol and dried at 60 °C. $Ce(III)$ chloride was added to the solution of *para* at a stoichiometric ratio of 1:3 and was synthesized by the same procedure.

Instruments

The elemental analyses of %C, %H and %N contents were performed by a microanalysis unit using a Perkin Elmer CHN 2400 analyzer. The molar conductivity of a freshly prepared 10^{-3} mol/cm³ dimethylsulfoxide (DMSO) solution of the dissolved complexes was measured using a Jenway 4010 conductivity meter. The electronic spectra were measured on UV-3101 PC Shimadzu UV-Vis spectrophotometer. The infrared spectra with KBr discs were recorded on a Bruker FT-IR spectrophotometer (4000–400 cm⁻¹). 1H -NMR spectra were scanned using a Varian Gemini 200 MHz spectrometer. The solvent used was DMSO. The thermal study TG/DTG-50H was carried out on a Shimadzu thermogravimetric analyzer under nitrogen atmosphere till 800 °C. The transmission electron microscopy images were recorded using a JEOL 100s microscope. Magnetic measurements were carried out on a Sherwood scientific magnetic balance in the micro analytical laboratory using Gouy method.

Antimicrobial effects

The biological activity of Ce^{3+} and Th^{4+} complexes of *diclo* and *para* drugs were tested against bacteria and fungi. In testing the antibacterial activity of these complexes, we used more than one test organism. The organisms used in the present investigation included two bacteria *B. subtilis* (Gram +), *E. coli* (Gram -) and two fungi *Aspergillus niger* and *Aspergillus flavus*. The results of the bactericidal and fungicidal screening of the synthesized complexes were collected.

RESULTS AND DISCUSSION

Microanalytical and conductance data

Selected physical properties and characteristic data of the synthesized metal complexes of *diclo* and *para* are listed in Table 1. The four new isolated solid complexes are formulated as $[Ce(diclo)_3] \cdot 2H_2O$, $[Th(diclo)_2(OH)_2] \cdot 4H_2O$, $[Ce(para)_3(H_2O)_3]$ and $[Th(para)_4(H_2O)_2]$. The complexes are air-stable, with high melting points. The metal complexes are insoluble in common organic solvents but are soluble in DMSO. The molar conductivity of 10^{-3} mol/dm³ solutions of the complexes in DMSO (Table 1) indicates that all synthesized complexes are non-electrolytes [28].

Table 1. Elemental analysis and physical data of *diclo* and *para* complexes with Ce(III) and Th(IV) metal ions.

Complexes	%C		%H		%N		%M		Δ (Ω^{-1} . cm ² .mol ⁻¹)
	Found	Calcd.	Found	Calcd.	Found	Calcd.	Found	Calcd.	
[Ce(<i>diclo</i>) ₃].2H ₂ O 1	47.44	47.52	3.20	3.23	3.90	3.96	13.16	13.20	15
[Th(<i>diclo</i>) ₂ (OH) ₂].4H ₂ O 2	36.12	36.22	3.21	3.26	2.98	3.02	24.90	24.99	19
[Ce(<i>para</i>) ₃ (H ₂ O) ₃] 3	44.56	44.72	4.58	4.69	6.44	6.50	21.65	21.74	21
[Th(<i>para</i>) ₄ (H ₂ O) ₂] 4	44.21	44.24	4.12	4.18	6.42	6.45	26.55	26.71	17

The synthesized complexes according to elemental analysis, IR, ¹H-NMR, UV-Vis and thermogravimetric data confirm that the complexes have monodentate and bidentate chelation for the *para* and *diclo* chelator, respectively. These data matched with the calculated elemental analysis revealing that no Cl⁻ ions were detected by addition of AgNO₃ reagent to the solution of the mentioned complexes.

Infrared spectra

The IR data of *diclo* and its Ce(III) and Th(IV) complexes are shown in Table 2 and Fig. 3. The IR spectra of these complexes were compared with those of the free *diclo* ligand in order to determine the coordination sites involved in chelation. It was observed in the IR spectra that there are no large shifts for ν (NH) and δ (NH) bands in the spectra of all complexes compared to those of the ligand, which indicates that there is no interaction between the -NH group and the metal ions. The difference between the bands of $\nu_{as}(\text{COO})$ and $\nu_s(\text{COO})$ characterized the carboxylate ligation. The $\nu_{as}(\text{COO})$ and $\nu_s(\text{COO})$ bands of the *diclo* complexes are at 1581-1546 and 1445-1423 cm⁻¹, respectively. The difference ($\Delta = \nu_{as}\text{COO} - \nu_s\text{COO}$) of 136-123 cm⁻¹ is

less than the ionic value of sodium diclofenac (the Δ value is 170 cm⁻¹), as expected for the bidentate bridging mode of carboxylate. Diclofenac complexes exhibit bands at 3782 and 3594 cm⁻¹ attributed to the presence of coordinated and lattice water [29]. The weak band at 570-528 cm⁻¹ of the complexes was assigned to the $\nu(\text{M-O})$ stretching vibration motion. The IR data of *para* and its Ce(III) and Th(IV) complexes are shown in Table 3 and Fig. 4. From the comparison of the IR spectra of *para* and its complexes, it follows that:

- The absorption bands at 3300 cm⁻¹ and 3200 cm⁻¹ of free *para* were assigned to -OH and -NH stretching vibration motions. These bands were shifted in the spectra of the metal complexes due to coordination.
- The strong absorption band at 680 cm⁻¹ in the spectra of the metal complexes which does not appear in the free *para* was tentatively assigned to [M-OH] stretch band of metal complex.
- The blue shift of stretching band and in-plane bend band of hydroxyl group, with respect to phenyl moiety at 1260-1100 cm⁻¹ is an evidence for the contribution of the hydroxyl oxygen atom to chelation with the metal ion.

Table 2. IR spectra of *diclo* and its Ce(III) and Th(IV) complexes

Compound	ν (NH) and ν (OH)	δ (NH)	ν (COO) (as)	ν (COO) (s)	ν (M-O) (COO)	Δ	ν (M-O) (H ₂ O)
<i>Diclo</i>	3359	1500	1572	1402	--	170	--
1	3776 3594 3250	1504	1546	1423	533	123	570
2	3782 3598 3321	1503	1581	1445	452	136	528

Table 3. IR frequencies (4000-400 cm⁻¹) of *para* and its Ce(III) and Th(IV) complexes.

Compound	ν (OH) + ν (NH)	ν (C=O)	δ (CNH) amide group	ν (C-O) phenyl group	ν (M-O)
<i>Para</i>	3300 3200	1650	1560	1260	--
3	3389	1620	1538	1200	509
4	3322 3160	1654	1560	1240	508

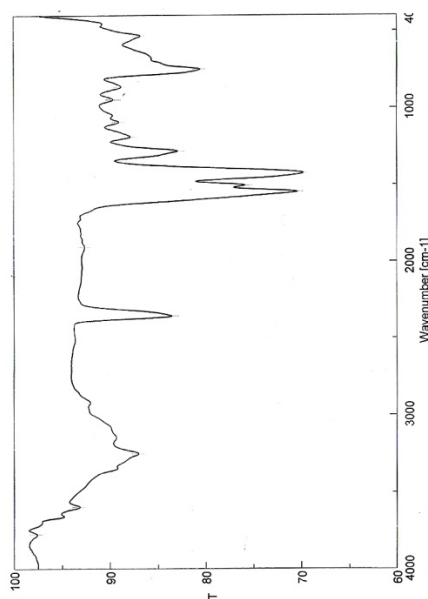


Fig. 3a. FT-IR spectrum of *diclo*/Ce³⁺ complex

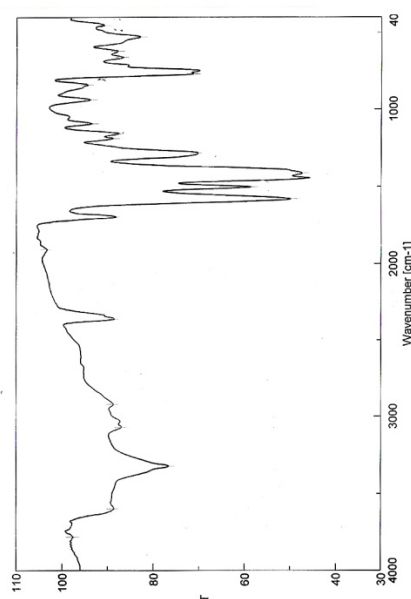


Fig. 3b. FT-IR spectrum of *diclo*/Th⁴⁺ complex

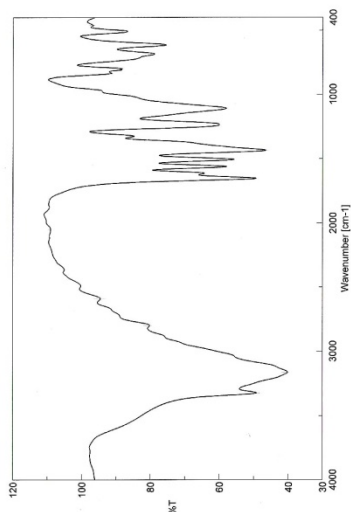


Fig. 4a. FT-IR spectrum of *para*/Ce³⁺ complex

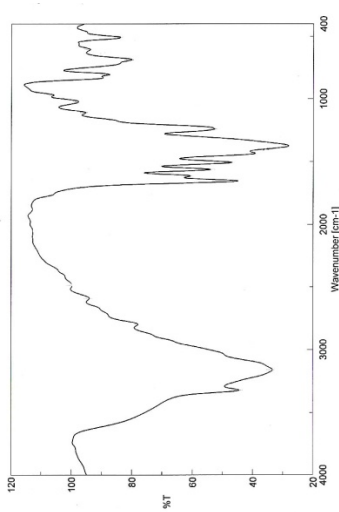


Fig. 4b. FT-IR spectrum of *para*/Th⁴⁺ complex

¹H-NMR spectra

The ¹H-NMR spectral data of *diclo* and its Th(IV) complex are presented in Table 4 and Fig. 5. The ¹H-NMR spectrum of the Th(IV) complex shows that the signals of the protons of the aromatic CH₂ and CH are unshifted at δ = 3.50 ppm as a broad singlet which refers to CH₂ of acetate group and proton of uncoordinated water. The multiplet peaks at 6.2-7.5 ppm were attributed to the protons of phenyl group

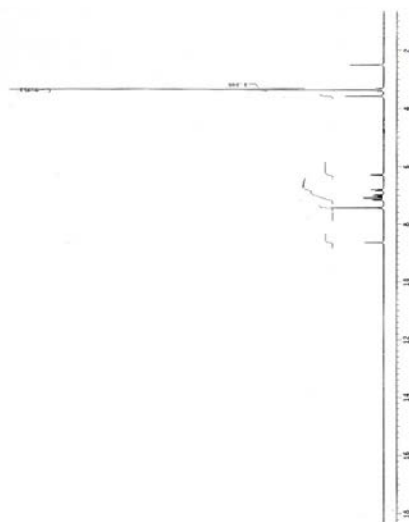
of two *diclo* molecules, in the prepared complex. The protons of both NH and OH of coordinated chelate appeared as a broad singlet at δ = 8.6 ppm in the spectrum of the Th⁴⁺ complex, thus, the upfield shift of the complex would mean coordination with a cleaved metal ion. The association is due to intermolecular hydrogen bond with respect to the pure salt [30-32].

Table 4. ¹H-NMR spectral data of *diclo* and its Th(IV) complex

Compound	δ(ppm) of protons			
	2H; H ₂ O	H; CH ₂	H; ArH	H; NH
<i>Diclo</i>	--	3.410	6.23-7.47	10.51
2	2.503	3.504	6.2-7.52	8.6

Table 5. $^1\text{H-NMR}$ spectral data of *diclo* and its Th(IV) complex.

Compound	δ ppm of hydrogen				
	H; CH_3	H; H_2O	H; ArH	H; NH	H; OH
<i>Para</i>	1.9	--	6.57-7.28	9.37	10
4	1.96	2.5	6.6-7.22	9.6	--

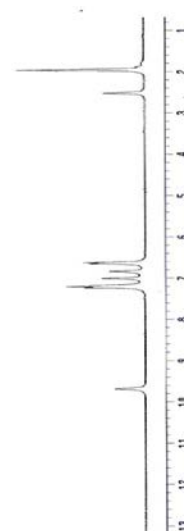
**Fig. 5.** $^1\text{H-NMR}$ spectrum of *diclo*/Th $^{4+}$ complex.

$^1\text{H-NMR}$ spectrum of *para* (Table 5) displays the signals $\delta = 9.37$ and 10.00 ppm which are due to the proton of the amide and hydroxyl groups, respectively. The disappearance of the signal $\delta = 10.00$ ppm of the hydroxyl hydrogen atom in the $^1\text{H-NMR}$ spectrum of the Th(IV) complex of *para* (Fig. 6) confirms the consumption of hydroxyl hydrogen atom in the complexation between *para* and metal ion. The persistence of the signal of the proton of the amide hydrogen atom in the $^1\text{H-NMR}$ spectrum of the complex confirms that amide proton does not participate in the complexation.

Magnetic measurements and UV-Vis spectra

The molar susceptibilities of thorium(IV) complexes (**2** and **4**) are diamagnetic, which agrees with the similar properties of other thorium(IV) complexes reported earlier [33,34]. The molecular weight data of the complexes also support this fact. Magnetic moment data show that lanthanum(III) nitrate complexes are essentially diamagnetic in nature while all other complexes are paramagnetic due to the presence of 4f-electrons which are effectively shielded by $5s^2p^2$ electrons [35]. This shows that 4f-electrons do not participate in the bond formation [36]. Magnetic moment data of the Ce(III) complexes of **1** and **3** are 2.77 and 2.84 B.M.

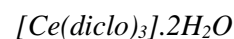
The formation of the metal complexes was also confirmed by UV-Vis spectra. The electronic spectra of the metal complexes in DMSO were scanned within the range of 200-600 nm. The free *diclo* drug has two essential bands; the first band at 275 nm may

**Fig. 6.** $^1\text{H-NMR}$ spectrum of *para*/Th $^{4+}$ complex

be attributed to $\pi-\pi^*$ transition of the aromatic ring and the second observed band at 350 nm - to $n-\pi^*$ electronic transition. In case of the spectra of metal complexes, the two bands are bathochemically shifted, suggesting that the ligand is coordinated to the metal ion through carboxylic group. It can be seen that free *para* has two distinct absorption bands. The first one at 300 nm may be attributed to $\pi-\pi^*$ intra-ligand transition of the aromatic ring. The second band observed at 390 nm was attributed to $n-\pi^*$ electronic transition. These bands are shifted after complexation.

Thermogravimetric analysis

Thermogravimetric analysis of the *diclo* complexes was performed and weight loss was measured from ambient temperature up to 1000°C . The decomposition behavior is shown in Fig. 7.



The thermal decomposition of this complex occur in four steps. The 1st step takes place in the range $60-170^\circ\text{C}$ and corresponds to the loss of $2\text{H}_2\text{O}$, with weight loss of 3.90% and its calculated value is 3.39%. The second step takes place in the range of $170-290^\circ\text{C}$ corresponding to the loss of two terminal Cl_2 molecules with weight loss of 6.83% and its calculated value is 6.69%. The third and fourth decomposition steps occur in the range of $290-900^\circ\text{C}$ and correspond to the loss of organic molecules. $\frac{1}{2}\text{Ce}_2\text{O}_3$ contaminated with residual carbon is the final product.

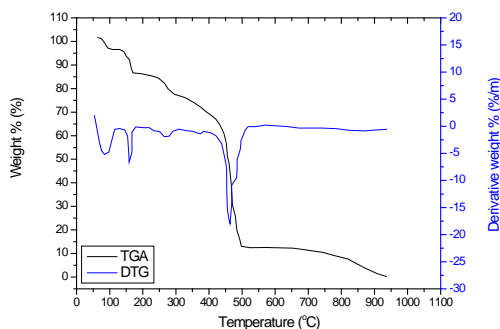


Fig. 7a. TG-DTG curves of *diclo*/ Ce^{3+} complex.

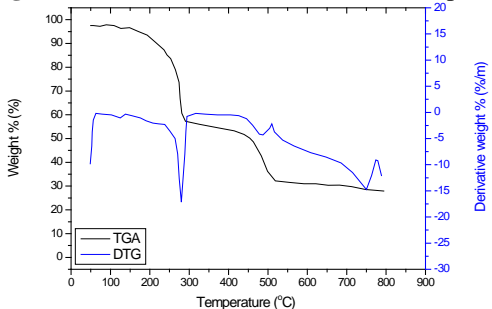
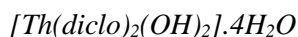
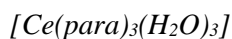


Fig. 7b. TG-DTG curves of *diclo*/ Th^{4+} complex.



The thermal decomposition of this complex occurs in four steps. The first decomposition step takes place in the range of 120-190°C and corresponds to the loss of 2H₂O molecules representing a weight loss of 2.50% and its calculated value is 1.94%. The 2nd step occurs in the range of 190-340°C, corresponding to the loss of two water molecules and decomposition of the organic moiety, representing a weight loss of 39.30% and its calculated value is 40%. The 3rd step takes place in the range of 340-490°C. It corresponds to the loss of the remaining organic molecules, representing a weight loss of 33.90% and its calculated value is 33.80%. The fourth step corresponds to the loss of organic molecules. The final product is ThO₂ oxide.

In case of *para* complexes, the heating rate was controlled at 10°C/min under nitrogen atmosphere and the weight loss was measured from ambient temperature up to \approx 1000 °C. The weight losses for each chelate was calculated within the corresponding temperature ranges (see Fig. 8).



The mentioned complex was decomposed in two essential steps: the first step occurs at 50-250°C and corresponds to the loss of 3H₂O and part of the organic molecules. The mass loss due to this step was 19.79% (obs.) and 20.21% (calcd.). The second step occurs at 250-600°C and corresponds to the loss of the remaining organic molecules with weight loss of 50.60% (obs.) and 50.88% (calcd.). The final product obtained at 800°C contained ½Ce₂O₃ and organic moiety.

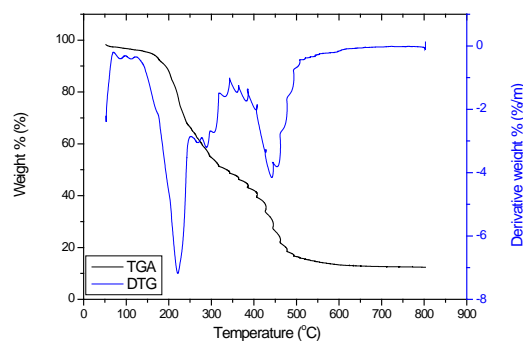


Fig. 8a. TG-DTG curves of *para*/ Ce^{3+} complex.

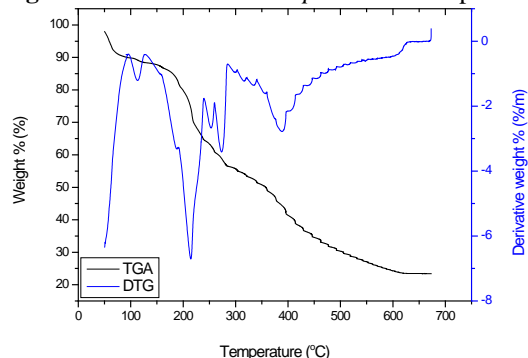
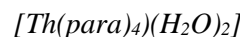


Fig. 8b. TG-DTG curves of *para*/ Th^{4+} complex.



The [Th(*para*)₄(H₂O)₂] complex was decomposed in three main steps. The first step takes place at 50-155°C and corresponds to the loss of 2H₂O molecules, representing a weight loss of 4.50% (obs.) and 4.14% (calcd.). The second step takes place within the temperature range 155-379°C and can be assigned to the loss of organic molecules of *para*, the mass loss due to this step was 31.90% (obs.) and 31.40% (calcd.). The third step occurs at 379-650°C and corresponds to the loss organic molecules of *para*, the mass loss due to this step was 53.00% (obs.) and 52.70% (calcd.). The final product at 750°C is ThO₂.

Kinetic thermodynamic calculations

The calculated thermodynamic parameters from TG and DTG are listed in Table 6. The thermodynamic activation parameters of the decomposition processes of the complexes, namely, activation energy (ΔE^*), enthalpy (ΔH^*), entropy (ΔS^*) and Gibbs free energy change of the decomposition (ΔG^*) were evaluated graphically (Figs. 7, 8) by employing the Coats-Redfern and Horowitz – Metzger relations [37, 38]. In order to access the influence of the structural properties of the ligand and the type of the metal on the thermal behavior of the complexes, the order, *n*, and the heat of activation *E* of the various decomposition stages were determined from the TG and DTG thermograms.

Table 6. Kinetic parameters using the Coats–Redfern (CR) equations for the complexes **1-4**.

Complex	Step	Kinetic Parameters					
		E (Jmol ⁻¹)	A (S ⁻¹)	Δ S (Jmol ⁻¹ K ⁻¹)	Δ H (Jmol ⁻¹)	Δ G (Jmol ⁻¹)	r
1	1 st	9.40E+04	7.34E+11	-1.90E+01	9.08E+04	9.65E+04	0.97104
2	1 st	4.66E+04	5.00E+04	-1.52E+02	4.36E+04	1.00E+05	0.97315
3	1 st	6.87E+04	1.30E+07	-1.20E+02	6.45E+04	1.20E+05	0.97021
4	1 st	5.15E+04	2.02E+05	-1.40E+02	4.70E+04	1.01E+05	0.97423

Coats – Redfern equation. The equations are as follows:

$$\ln \left[\frac{1 - (1 - \alpha)^{1-n}}{(1-n)T^2} \right] = \frac{M}{T} + B \quad \text{for } n \neq 1 \quad (1)$$

$$\ln \left[\frac{-\ln(1 - \alpha)}{T^2} \right] = \frac{M}{T} + B \quad \text{for } n = 1 \quad (2)$$

where $M = -E/R$ and $B = \ln AR/\Phi E$; E , R , A , and Φ are the heat of activation, the universal gas constant, pre-exponential factor and heating rate, respectively. The correlation coefficient, r , was computed using the least square method for different values of n , by plotting the left-hand side of Eqs. (1) or (2) versus $1000/T$.

Horowitz – Metzger equation. The relations derived are as follows:

$$\ln [-\ln(1 - \alpha)] = \frac{E}{RT_m} \Theta \quad (3)$$

where α , is the fraction of the sample decomposed at time t and $\Theta = T - T_m$.

The plot of $\ln [-\ln(1 - \alpha)]$ against Θ was found to be linear, from the slope of which E was calculated and Z can be deduced from the relation:

$$Z = \frac{E\phi}{RT_m^2} \exp \left(\frac{E}{RT_m} \right) \quad (4)$$

where ϕ is the linear heating rate, the order of reaction, n , can be calculated from the relation:

$$n = 33.64758 - 182.295\alpha_m + 435.9073\alpha_m^2 - 551.157\alpha_m^3 + 357.3703\alpha_m^4 - 93.4828\alpha_m^5$$

The n value which gave the best fit ($r \approx 1$) was chosen as the order parameter for the decomposition stage of interest. From the intercept and linear slope of such stage, the A and E values were determined. The other kinetic parameters, ΔH , ΔS and ΔG were computed using the relationships; $\Delta H = E - RT$, $\Delta S = R[\ln(Ah/kT) - 1]$ and $\Delta G = \Delta H - T\Delta S$, where k is the Boltzmann constant and h is the Planck constant. The following remarks can be pointed out: (i) all complexes decomposition stages show a best fit for ($n = 1$) indicating a first-order decomposition in all cases. Other n values (e.g. 0, 0.3 and 0.7) did not lead to better correlations [39,40]; (ii) the negative values

of activation entropies ΔS indicate a more ordered activated complex than the reactants and/or slow reactions [41]; (iii) the positive values of ΔH mean that the decomposition processes are endothermic.

Transmission electron microscopy

The surface morphology and particle size of all *diclo* and *para* complexes were obtained from transmission electron micrography (TEM) (Fig. 9a-d). It is clear that these complexes have uniform matrix and homogeneity. The surface morphology of the TEM micrograph reveals the well sintered nature of the complexes with varying grain sizes and shapes. Clear large grains are obtained with agglomerates for all complexes. The distribution of the grain size is homogeneous except that medium to small particles of size about 200 nm-0.5 μm are obtained.

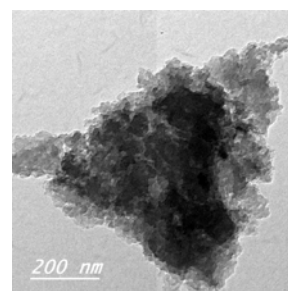


Fig. 9a. TEM image of *diclo*/Ce³⁺ complex.

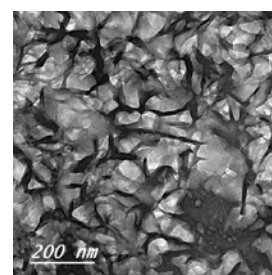


Fig. 9b. TEM image of *diclo*/Th⁴⁺ complex.

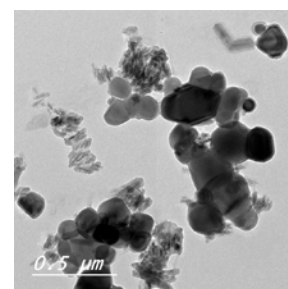


Fig. 9c. TEM image of *para*/Ce³⁺ complex.

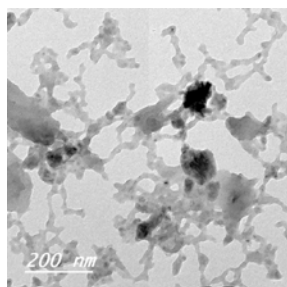


Fig. 9d. TEM image of *para*/Th⁴⁺ complex.

3-8-Antimicrobial activity

Antibacterial and antifungal activity of the *diclo* ligand and its complexes are carried out against two kind of bacteria, *B. subtilis* (Gram +ve), *Escherichia coli* (Gram -ve) and fungal (*Aspergillus niger*, *Aspergillus flavus*) in Fig. (10) and Table 7. The antimicrobial activity estimated based on the size of inhibition zone around dishes. The complexes are found to have high activity against *Aspergillus niger* and *flavus*.

Antibacterial and antifungal activities of *para* complexes were studied against bacteria (Gram-) as *Escherichia coli*, (Gram +) as *Bacillus subtilis* and

fungi (*Aspergillus niger* and *Aspergillus flavus*). The antimicrobial activity was estimated based on the size of the inhibition zone in the dishes. Th(IV) complex was found to have high activity against bacteria and the two kinds of fungi. The data are shown Table 8 and Fig. 10.

Suggested structures of Ce(III) and Th(IV) complexes

The structures of the complexes of *diclo* and *para* drugs with Ce(III) and Th(IV) metal ions were confirmed by elemental analysis, IR, molar conductance, UV-Vis, ¹H-NMR and thermal analysis data.

Thus, from ¹H-NMR and IR spectra, it was concluded that *diclo* chelated in a bidentate fashion but *para* behave as monodentate ligand coordinated to the metal ion *via* the oxygen of the phenolic group. From the molar conductance data, it was found that all complexes seem to be non-electrolytes. So, the investigated complexes have the structures shown in Fig. 11.

Table 7. Antimicrobial effect of *diclo* complexes.

	Diameter of inhibition zone (cm)			
	<i>B. subtilis</i>	<i>E. coli</i>	<i>Aspergillus niger</i>	<i>Aspergillus flavus</i>
Control	0	0	0	0
<i>Diclo</i> /Ce	2	1.2	2.2	2.3
<i>Diclo</i> /Th	1.8	1	2.2	2.2

Table 8. Antimicrobial effect of *para* complexes.

	Diameter of inhibition zone (cm)			
	<i>B. subtilis</i>	<i>E. coli</i>	<i>Aspergillus niger</i>	<i>Aspergillus flavus</i>
Control	0	0	0	0
Ce(III) complex	1.3	1.1	2.6	1.8
Th(IV) complex	1.7	1.2	1.7	3.1

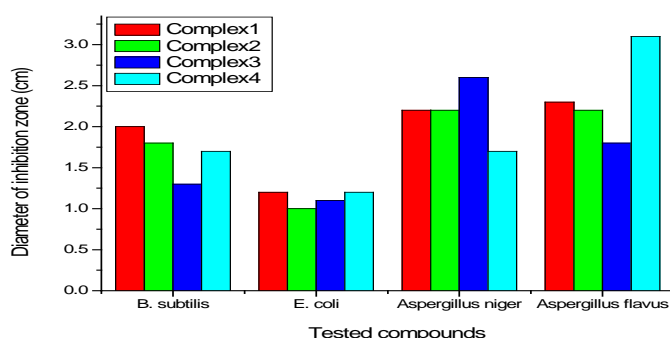
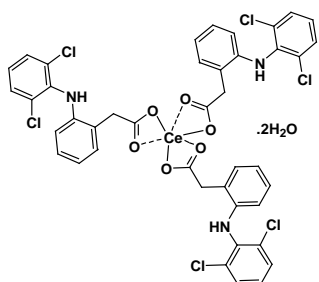
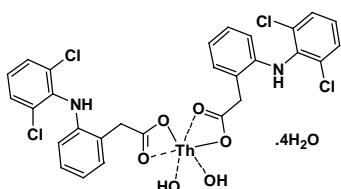


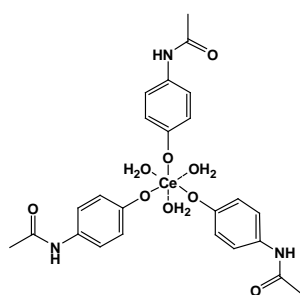
Fig. 10: Statistical representation of the biological activity of complexes 1-4.



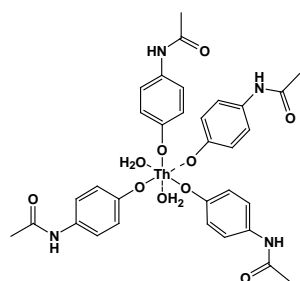
Complex 1



Complex 2



Complex 3



Complex 4

Fig. 11. Structure of the investigated complexes.

REFERENCES

- M. Tuncay, S. Calis, H.S. Kas, M.T. Ercan, I. Peksoy, A.A. Hincal, *Int. J. Pharm.*, **195**, 179 (2000).
- D. Kovala-Demertzi, D. Mentzafos, A. Terzis, *Polyhedron*, **12**, 1361(1993).
- M.E. Abdel-Hamid, L. Novotony, H. Hamza, J. *Pharm. Biomed. Anal.*, **24**, 587 (2001).
- P.A. Todd, E.M. Sorkin, *Drugs*, **35**, 244 (1988).
- P. Moser, A. Sallmann, I. Wiesenberg, *J. Med. Chem.*, **33**, 2358 (1990).
- W.D. Horrocks. D.R. Sundnick, *J. Am. Soc.*, **101** 334 (1979).
- J. R. Vane, R.M. Botting, *Inflamm. Res.*, **1** (1995).
- C. Castellari, S. Ottani, *Acta. Crystallogr.*, **53** 794 (1997).
- M.R. Caira, V.J. Griggith, L.R. Outshoorn Massimbeni, *J. Chem Soc., Chem Commun.*, **9** 1061 (1994).
- I. Bratu, S. Astilean, C. Lonesc, J.P. Indrea, J.P. Huvenne P. Legrand, *Spectrosc. Acta Part A*, **54** 191 (1998).
- M.A. Jan Mens, *Best Pract. Res. Clin. Rheumat.*, **19**, 609 (2005).
- E. Dic, A. Ozdemir, D. Baleanu, *Talanta*, **65** 36 (2005).
- A.B. Moreira, H.B.M. Oliveira, T.D.Z. Atvars, L.L.T. Dias, G.O. Neto, E.A.G. Zagatto, L.T. Kubota, *Anal. Chim. Acta*, **539**, 257 (2005).
- B.B. Ivanova, *J. Mol. Struct.*, **738**, 233 (2005).
- C. Xu, B. Li, *Spectrochim. Acta A*, **60**, 1861 (2004).
- L.G. Binev, Y.I. Vassileva-Boyardjieva, J. Binev, *Mol. Struct.*, **447** 235 (1998).
- A.M. MacConnachie, *Intensive Crit. Care Nuts*, **13**, 238 (1997).
- J.L. Vilchez, R. Blance, R. Avidad, A. Navalon, J. *Pharm. Biomed.* **13** (1995) 119.
- D. Easwaramoorthy, Y. Yu, H. Huang, *Anal. Chim. Acta*, **439**, 95 (2001).
- H. Tanka, P.K. Dasgupta, J. Huang, *J. Anal. Chem.*, **72**, 4713 (2000).
- J.P. Shockcor, S.E. Linger, I.D. Wilson, *Anal. Chem.*, **68**, 4431 (1996).
- S. Murray, A.R. Boobis, *J. Chromatogr.*, **33**, 355 (1991).
- A.K. Singh, R. Negi, Y. Katre, S.P. Singh, *Journal of Molecular Catalysis A: Chemical*, **302**, 36 (2009).
- L.F. Prescott, Paracetamol overdose. Pharmacological consideration and clinical management, *Drugs*, **25**, 290 (1983).
- P.J. Harvison, F.P. Guengerich, *Chem. Res. Toxicol.*, **1**, 47 (1988).
- L. Chavkin, H. Merkle, US Patent (1979).
- F.J. Strenbenz, L. Weintraub, G.L. Cohen, UK Patent, Application GB 2103 87A, 1983.
- W.J. Geary, *Coord. Chem. Rev.*, **7**, 81 (1971).
- K. Nakamoto, *Infrared and Raman Spectra of Inorganic and Coordination Compounds: Part B*, 5th ed., Wiley, New York, 1997.
- D. Kovala-Demertzi, S.K. Hadjikakou, M.A. Demertzis, Y. Deligiannakis, *Journal of Inorganic Biochemistry*, **69**, 223 (1998).
- D. Kovala-Demertzi, A. Theodorou, M.A. Demertzis, C.P. Raptopoulou, A. Terzis, *Journal of Inorganic Biochemistry*, **65**, 151 (1997).
- D. Kovala-Demertzi, D. Mentzafos, A. Terzis, *Polyhedron*, **12** 1361 (1993).
- B.B. Misra, S.R. Mohanty, N.V.V.S. Murti, S. Roychowdhury, *Inorg. Chim. Acta*, **28**, 275 (1978).
- E.D. Eastman, L. Brawar, L.A. Bromby, P.W. Gilles, N.L. Lofgren, *J. Am. Chem. Soc.*, **72**, 4019 (1950).
- R.K. Agarwal, Himanshu Agarwal, *Synth React Inorg Met Org Chem.*, **31**, 263 (2001).
- P. Indersenan, Raj N. K. Kala, *J. Indian Chem. Soc.*, **77**, 259 (2000).

37. A. W. Coats, J. P. Redfern, *Nature*, **201**, 68 (1964).
38. H. W. Horowitz, G. Metzger, *Anal. Chem.*, **35** 1464 (1963)
39. P.B. Maravalli, T.R. Goudar, *Thermochim. Acta*, **325**, 35 (1999).
40. K.K.M. Yusuff, R. Sreekala, *Thermochim. Acta*, **159**, 357 (1990).
41. A.A. Frost, R.G. Pearson, *Kinetics and Mechanisms*, Wiley, New York, 1961.

НОВИ ХЕЛАТНИ ПРОДУКТИ НА ТОРИЙ(IV) И ЦЕРИЙ(III) С АНАЛГЕТИЧНИТЕ ЛЕКАРСТВА ДИКЛОФЕНАК И ПАРАЦЕТАМОЛ: СИНТЕЗ И ИЗСЛЕДВАНЕ НА СПЕКТРОСКОПСКИТЕ ХАРАКТЕРИСТИКИ, ТЕРМИЧНАТА СТАБИЛНОСТ И АНТИМИКРОБИАЛНАТА АКТИВНОСТ

Ф.А.И. Ал-Кодир

Департамент по химия, Научен колеж, Университет Принцеса Нора Бинт Абдул Рахман

Постъпила на 26 ноември, 2017 г.; Коригирана на 21 декември 2017 г.

(Резюме)

Четири нови комплекса на торий(IV) и церий(III) с две аналгетични лекарства, натриев диклофенак (*diclo*) и парацетамол (*para*): $[\text{Ce}(\text{diclo})_3] \cdot 2\text{H}_2\text{O}$ (1), $[\text{Th}(\text{diclo})_2(\text{OH})_2] \cdot 4\text{H}_2\text{O}$ (2), $[\text{Ce}(\text{para})_3(\text{H}_2\text{O})_3]$ (3), и $[\text{Th}(\text{para})_4(\text{H}_2\text{O})_2]$ (4), са синтезирани и охарактеризирани чрез елементарен анализ, термичен анализ, FT-IR, $^1\text{H-NMR}$ и UV-VIS спектроскопия. Микроаналитичното определяне на елементите показва, че съотношението метал:лекарство за синтезираните комплекси е съответно 1:3 за комплексите 1 и 3, 1:4 за комплекс 2 и 1:2 за комплекс 4. Вибрациите на разтягане $\nu_s(\text{O-H})$ на $-\text{OH}$ във FT-IR спектрите на *para* лиганда изчезват в спектрите на комплексите, което доказва включването на кислорода от $-\text{OH}$ групата в комплексообразуването след депротониране. При *diclo* комплексите, вибрациите на разтягане $\nu(\text{C=O})$ на карбоксилната група се изместват в спектрите на комплексите, което потвърждава включването на $-\text{COOH}$ групата в комплексообразуването с ковалентно свързване като бидентатно хелатообразуване. Геометрията на Ce^{3+} и Th^{4+} йони в комплексите с лекарствата е шест-координирана. Наноструктурните форми са изследвани с помощта на трансмисионна електронна микроскопия. Антимикробните свойства на новосинтезираните комплекси са определени спрямо някои видове бактерии и гъбички. Всички синтезирани комплекси притежават антимикробна активност.